ELSEVIER

Surface Science 314 (1994) L937–L942

surface science

Surface Science Letters

Scaling of heteroepitaxial island sizes

C. Ratsch [a], A. Zangwill [a,*], P. Šmilauer [b,1,2]

[a] *Interdisciplinary Research Centre for Semiconductor Materials, Imperial College, London SW7 2BZ, UK*

[b] *School of Physics, Georgia Institute of Technology, Atlanta, GA 30332, USA*

Received 28 February 1994; accepted for publication 24 May 1994

Abstract

Monte Carlo simulations of an atomistic solid-on-solid model are used to study the effect of lattice misfit on the distribution of two-dimensional islands sizes as a function of coverage θ in the submonolayer aggregation regime of epitaxial growth. Misfit promotes the detachment of atoms from the perimeter of large pseudomorphic islands and thus favors their dissolution into smaller islands that relieve strain more efficiently. The number density of islands composed of s atoms exhibits scaling in the form $N_s(\theta) \sim \theta/\langle s\rangle^2 g(s/\langle s\rangle)$ where $\langle s\rangle$ is the average island size. Unlike the case of homoepitaxy, a rate equation theory based on this observation leads to qualitatively different behavior than observed in the simulations.

The morphology that obtains when atoms of one material are deposited onto a substrate of a dissimilar material is a central concern in current efforts to fabricate nanostructures in situ during growth. Equilibrium considerations make clear that small, undislocated, three-dimensional islands achieve significant epitaxial strain relief by lattice relaxation at the island edges [1]. But such relaxation occurs at the edges of two-dimensional (2D) heteroepitaxial islands as well [2]. Thus, since there is evidence that 2D islands form a template from which 3D island structures evolve [3], it seems appropriate to focus attention on some of the kinetic aspects of heteroepitaxy even before a full monolayer has been deposited. To this end, we study here the evolution of 2D island size distributions with a simple simulation model of epitaxial growth suited to the case when the difference between the deposited material and the substrate is completely characterized by their lattice misfit.

The computations reported here generalize a previously successful Monte Carlo model of homoepitaxy [4]. There, atoms are deposited at random onto the (001) surface sites of a simple cubic lattice (with unit lattice constant) at an average rate F. No vacancies or overhangs are permitted, but any surface atom can hop to any nearest neighbor site at a rate $D\exp(-nE_N/k_BT)$, where $D = (2k_BT/h)\exp(-E_S/k_BT)$ is the single adatom migration rate, E_N is an effective pair bond energy, and $n = 0$–4 is the number of lateral nearest neighbors before the hop occurs.

* Corresponding author. Fax: +1 301 926 2746; E-mail: zangwill@zang1.gatech.edu.

[1] Also at: The Blackett Laboratory, Imperial College, London SW7 2BZ, UK.

[2] On leave from: The Institute of Physics, Czech Academy of Science, Cukrovarnická 10, 16200 Praha 6, Czech Republic.

SSDI 0039-6028(94)00325-4

In the present work, the deposition and zero-strain hopping rates are fixed by the choices $T = 750\,\mathrm{K}$, $F = 0.1\ \mathrm{s}^{-1}$, $E_S = 1.3$ eV, and $E_N = 0.3$ eV so that the dimensionless ratio $D/F = 6 \times 10^5$. All results represent an average of at least 50 realizations on a lattice of size 300×300.

We suppose [5] that the principal effect of strain is to lower the barrier to detachment of atoms from a strained pseudomorphic island. In a mean field picture, one might choose the barrier reduction to be identical for all atoms in an island and equal to the average strain energy per atom of that island. But since strain relief occurs primarily at the island edges we instead adopt a scheme whereby the strain-driven barrier reduction depends on the local coordination number [6]. More precisely, we make the replacement $E_N \rightarrow E_N - \mathcal{E}(\sqrt{s})$ for the atoms of an island composed of s atoms where $\mathcal{E}(m)$ is the energy per atom of a one-dimensional chain of m harmonically coupled atoms in contact with a rigid sinusoidal potential [7]. This choice exploits numerical results obtained from a fully 2D version of this model [8] which demonstrate that the energy density of a square island is well approximated by summing the energy density from two orthogonal *non-interacting* chains of atoms. Fig. 1 shows a log–log plot of the strain-induced Arrhenius factor $\Lambda_s = \exp[\mathcal{E}(\sqrt{s})/k_B T]$ with model parameters chosen to reproduce the elastic and cohesive properties of typical semiconductors [1].

The main effect of strain is to promote the dissolution of large islands by atom detachment [9]. This is most evident from a plot of the number density of 2D islands of size s, $N_s(\theta)$, at fixed coverage for different values of misfit (Fig. 2). Note that the monomer population is not the only beneficiary of the detachment process. Dimers and other small islands form rapidly but do not dissociate at an accelerated rate because they are relatively unstrained. The size distribution thus both narrows and shifts toward smaller islands sizes. More generally, we find that the average island size progressively decreases as misfit increases at fixed coverage. We note in passing that, compared to homoepi-

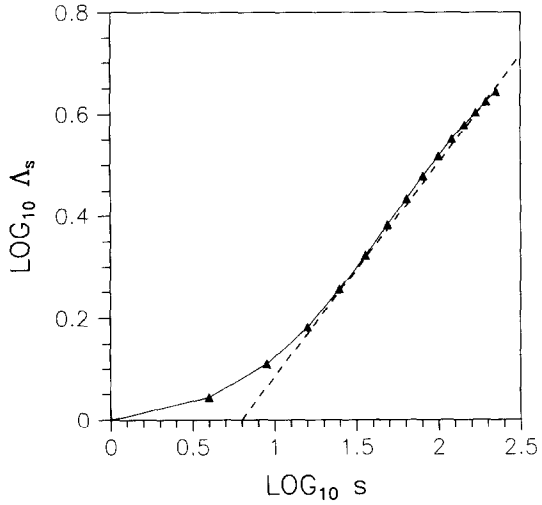

Fig. 1. Log–log plot of the island size dependence of the strain-induced Arrhenius factor $\Lambda_s = \exp[\mathcal{E}(\sqrt{s})/k_B T]$. The solid symbols denote values obtained analytically as described in the text. The straight dashed line is the power law approximation to it used in the rate equation analysis.

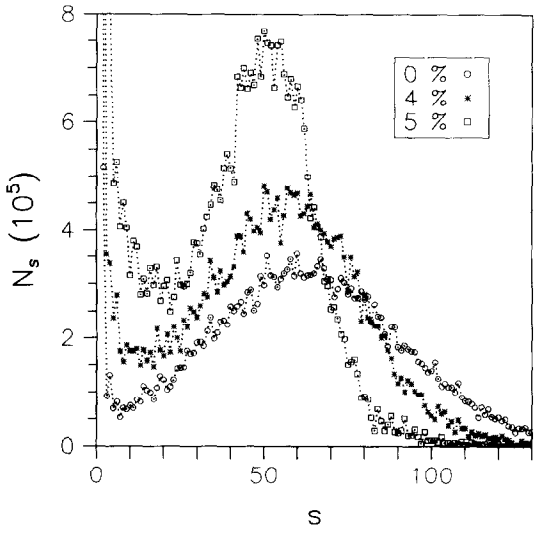

Fig. 2. Distribution of island sizes for different values of misfit f after 0.15 monolayers have been deposited. Results were obtained at $T = 750$ K with $F = 0.1\ \mathrm{s}^{-1}$, $E_S = 1.3$ eV, and $E_N = 0.3$ eV.

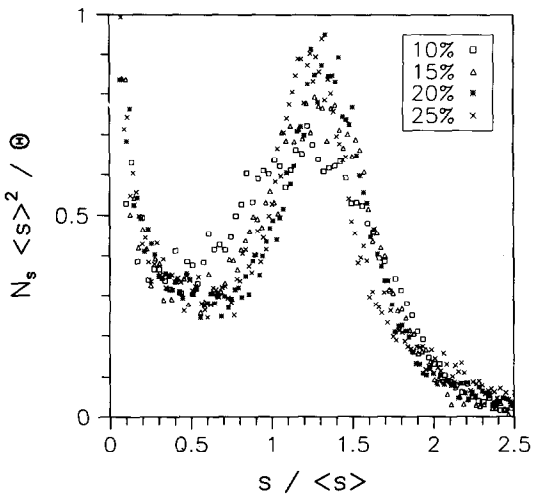

Fig. 3. Typical data collapse for 5% misfit. The data shown represent coverages from 10% to 25%.

taxy under otherwise identical conditions, this observation implies that relatively *better* layer-by-layer growth of strained material may be achieved so long as kinetic barriers inhibit strain-driven 3D islanding or misfit dislocation generation. This is so because the probability to nucleate next-layer islands onto the surface of existing islands decreases very sharply as their size decreases [10].

For the case of *homoepitaxy*, it is well established [11–15] that the island size distribution at low coverage is described by

$$N_s(\theta) \sim \frac{\theta}{\langle s \rangle^2} g\left(\frac{s}{\langle s \rangle}\right), \tag{1}$$

where $g(x)$ is a scaling function and $\langle s \rangle$ is the average island size. To test (1) for the case of *heteroepitaxy*, we plot $N_s \langle s \rangle^2 / \theta$ versus $s/\langle s \rangle$ and ask whether the simulation data at different coverages all collapse onto a single curve. That this is indeed the case [16] is illustrated in Fig. 3 for 5% misfit and $10\% \leq \theta \leq 25\%$. Similar scaling is found for other values of misfit so that, quite generally, the moments of the island size distribution are given by

$$M_n = \sum_s s^n N_s \sim \theta \langle s \rangle^{n-1} \int x^n g(x)\, dx. \tag{2}$$

To make progress, we require the coverage dependence of $\langle s \rangle$. The simulations reveal that this quantity is an increasing but not particularly simple function of θ for all values of misfit. But in the limited coverage range noted above, it turns out that the power law

$$\langle s \rangle \sim \theta^z, \tag{3}$$

represents the data well. The misfit-dependence of the exponent z can be extracted directly from (3) (square symbols in Fig. 4a) or from the coverage dependence of the density of all islands combined (dashed curves in Fig. 5) since, from (2), the latter quantity takes the form $N(\theta) = M_0 \sim \theta^{1-z}$ in the coverage range of interest. The triangles in Fig. 4a show that the two methods yield consistent results.

To understand the observed monotonic decrease of z toward zero it is convenient to return to the full $N(\theta)$ curves in Fig. 5. For our choice of deposition conditions, $N(\theta)$ grows very rapidly independent of misfit below about 1.5% coverage. New island formation then slows dramatically since the existing islands efficiently capture newly deposited adatoms. But the strain energy per atom increases as the islands grow and ejection of atoms from perimeter sites eventually ensues. Since the ejection rate increases as misfit increases, the nucleation rate of new islands from this source material increases similarly. Comparison with the zero-strain case in Fig. 5 reveals the efficacy of this process.

The coverage dependence of the number density of adatoms $N_1(\theta)$ is shown in Fig. 5 as well. The origin of the relative increase in this quantity as a function of misfit is clear from the foregoing. More interestingly, this quantity is seen to exhibit a power law variation

$$N_1(\theta) \sim \theta^{-r}, \tag{4}$$

in the same coverage interval where z was defined. Fig. 4b illustrates the misfit dependence of the exponent r extracted from the solid curves in Fig. 5 [17]. The obvious question now arises: can a simple theory be constructed that *predicts* the values for the exponents z and r? Previous simulation experience with aggregation-

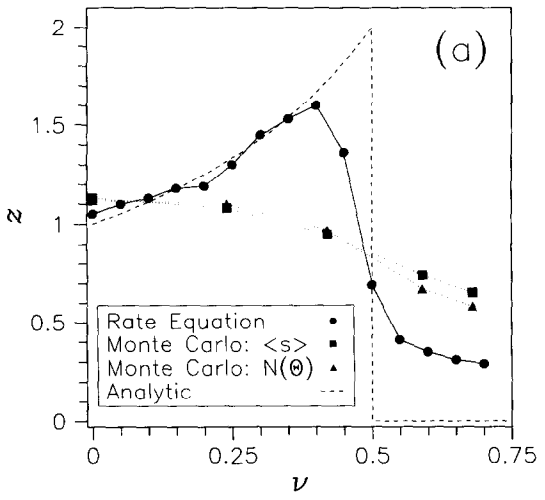

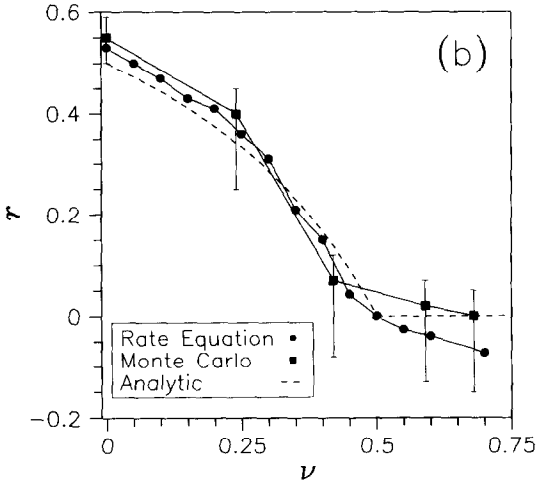

Fig. 4. Misfit dependence of the exponents z and r. Results are shown from the Monte Carlo simulations at 0%, 3%, 4%, 4.7%, and 5% misfit for $10\% \leq \theta \leq 25\%$ (squares and triangles), an analytic analysis of the rate equations (dashed lines), and a numerical solution of the rate equations (circles). The parameters ν and the misfit f are related through $\nu \simeq 0.027 f^2$.

fragmentation phenomena suggests that rate equation theory may be adequate for this purpose [18]. To this end, we write an evolution equation for the number density of each island species in the form [19]

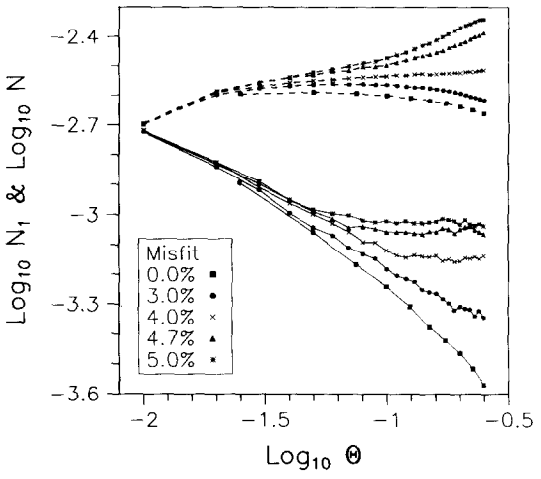

Fig. 5. Coverage dependence of the number density of adatoms $N_1(\theta)$ (solid curves) and the number density of all other island species combined $N(\theta)$ (dashed curves) for different values of misfit.

$$\frac{dN_1}{d\theta} = 1 - K_1 N_1^2 - N_1 \sum_{s\geq 1} K_s N_s + \gamma_2 N_2 + \sum_{s>1} \gamma_s N_s, \qquad (5)$$

$$\frac{dN_s}{d\theta} = N_1 (K_{s-1} N_{s-1} - K_s N_s) - \gamma_s N_s + \gamma_{s+1} N_{s+1}, \qquad (s > 1). \qquad (6)$$

These mean-field equations presume that only monomers are mobile and that islands grow and dissociate exclusively by the attachment and detachment of single monomers. The rate at which adatoms *attach* to an island of size s is assumed to take the form $K_s = K_0 s^p$ where, e.g., the exponent $p = 1/2$ for the present case of 2D compact islands [19]. Similarly, the rate at which adatoms *detach* from an island of size s takes the form $\gamma_s = \gamma_0 s^\nu$ for all but the very smallest islands. The exponent ν is deduced from plots similar to Fig. 1 to be $\nu \simeq 0.027\langle n\rangle f^2$ where $\langle n\rangle$ is the average coordination number of the detaching species and the lattice misfit f is expressed in percent. For our choice of E_N, $1 \leq \langle n\rangle \leq 2$, but we set $\langle n\rangle = 1$ in what follows since the precise value of the coefficient of f^2 anyway

depends on the material parameters used in the model calculation of $\mathcal{E}(\sqrt{s})$.

An exact equation of motion for the moments of N_s follows immediately from (2), (5) and (6):

$$\frac{dM_n}{d\theta} = \sum_s ((s+1)^n - s^n)(K_s N_1 N_s + \gamma_s N_s) - \gamma_2 N_2 + K_1 N_1^2 + \frac{dN_1}{d\theta}. \quad (7)$$

But we are interested in a solution at large times only so it is valid to neglect low order moments and the last three terms on the right hand side of (7). This yields the approximate expression

$$\frac{dM_n}{d\theta} \simeq nK_0 N_1 M_{n+p-1} - n\gamma_0 M_{n+\nu-1}. \quad (8)$$

When (2) is inserted into (8), we obtain the following self-consistent solutions for the desired exponents

$$r = z(p - \nu) \quad (9)$$

with

$$z = \begin{cases} (1-\nu)^{-1} & 0 \le \nu < p, \\ 0 & \nu > p. \end{cases}$$

Note that z is indeterminate for the case $p = \nu$. Otherwise, the values computed from (9) are plotted as dashed curves in Fig. 4 for comparison with the Monte Carlo values.

It is obvious that the prediction for the monomer exponent r show the same trend as the simulation results while the exponent z disagrees qualitatively. Presumably, the non-analytic behavior of (9) is an artifact of the simplifications required to derive (8). But are these approximations also responsible for the disagreement between the simulations and the rate equations regarding the behavior of z? To test this, we solved (5) and (6) numerically using rate parameters identical to those used in the simulations. Scaling of the assumed form does occur – but only at larger times (than found from the simulations) where coalescence should be important. Be that as it may, the qualitative behavior predicted by (9) is confirmed albeit with the discontinuities smoothed out (Fig. 4).

Quantitatively, our numerical integration confirms a recent prediction by Blackman and Marshall [20] that $r = 0$ and $z = 1/(2 - \nu)$ for the case $\nu = p$. Otherwise, our prediction that $r = z = 0$ when $\nu > p$ agrees with that of Ref. [20] but our result that $z > 1$ when $\nu < p$ is not consistent with these authors conclusion that "gelation takes place with the formation of an infinite cluster" in that regime. In any event, comparison with the Monte Carlo results clearly impel us to conclude that the failure of the rate equations to reproduce the exponent z extracted from the simulations is a real effect.

In the simulations (and in reality) an atom that detaches from an island generally remains close to that island and re-attaches to it with a high probability. But in the rate equation treatment, an adatom that detaches from an island becomes available for capture by all islands. Moreover, since larger islands capture more efficiently ($p > 0$), the average island size will grow at an exaggerated rate if monomers are in sufficient supply. Since increasing misfit precisely has the effect of generating monomers (cf. Fig. 5), (3) implies that z will increase over its homoepitaxy value. When $\nu > p$, atoms are ejected from larger islands at a higher rate than they are captured, many small islands form, and z decreases precipitously. Eventually, the strain-induced reduction in the detachment barrier exceeds the pair bond energy E_N and all islands disintegrate to yield adatoms as the only adsorbed species ($z \to 0$).

The present results can be combined usefully with the fact that rate equation predictions for homoepitaxy are satisfied quantitatively only for very large values of D/F [11,15,21]. Both results suggest that the theory is valid only when the number density of monomers is sufficiently small that the error associated with assigning equal capture efficiency to all islands of the same size is negligible. This observation might help guide future research directed to the formulation of an improved rate equation description of the present problem.

Acknowledgement

Dimitri Vvedensky kindly made available the computing resources used to perform the simulations. We thank John Blackman for a prepublication copy of Ref. [20] and Klaus Kern for an insightful remark on heteroepitaxial layer growth. This work was supported by the US Department of Energy, a NATO travel grant and the Research Development Corporation of Japan.

References

[1] See, e.g.: C. Ratsch and A. Zangwill, Surf. Sci. 293 (1993) 123 and references therein.
[2] J. Massies and N. Grandjean, Phys. Rev. Lett. 71 (1993) 1411.
[3] For the case of Fe(001) homoepitaxy, 2D island separations established in the submonolayer regime [J.A. Stroscio, D.T. Pierce and R.A. Dragoset, Phys. Rev. Lett. 70 (1993) 3615] are observed to be directly related to 3D island separations evident after 600 layers of growth [J.A. Stroscio and D.T. Pierce, unpublished].
[4] S. Clarke and D.D. Vvedensky, J. Appl. Phys. 63 (1988) 2272;
T. Shitara, D.D. Vvedensky, M.R. Wilby, J. Zhang, J.H. Neave, and B.A. Joyce, Phys. Rev. B 46 (1992) 6815, 6825.
[5] C. Ratsch and A. Zangwill, Appl. Phys. Lett. 63 (1993) 17.
[6] Simulation results using a related (but quite different) scheme to incorporate strain effects have been reported by N. Grandjean and J. Massies, J. Cryst. Growth 134 (1993) 51.
[7] J.H. Van der Merwe and C.A.B. Ball, in: Epitaxial Growth, Part B, Eds. J.W. Matthews (Academic Press, New York, 1980) Ch. 8.
[8] J.A. Snyman and J.H. Van der Merwe, Surf. Sci. 45 (1974) 619.
[9] This may be compared with a fission-like mechanism observed in molecular dynamics simulations of submonolayer Ag/Pt(111) at much higher temperature: P. Blandin, C. Massobrio and P. Ballone, Phys. Rev. Lett. 72 (1994) 3072.
[10] J. Tersoff, A.W. Denier van der Gon and R.M. Tromp, Phys. Rev. Lett. 72 (1994) 266.
[11] M.C. Bartelt and J.W. Evans, Surf. Sci. 298 (1993) 421; Phys. Rev. B 46 (1992) 12675.
[12] J.A. Stroscio and D.T. Pierce, Phys. Rev. B 49 (1994) 8522.
[13] C. Ratsch, A. Zangwill, P. Šmilauer and D.D. Vvedensky, Phys. Rev. Lett. 72 (1994) 3194.
[14] G.S. Bales and D. Chrzan, unpublished.
[15] J.G. Amar, F. Family and P.-M. Lam, unpublished.
[16] For the case of homoepitaxy [11], data collapses of this sort improve as the magnitude of the ratio D/F increases.
[17] The error bars in Fig. 4b indicate that the square symbols should be regarded as upper bounds to the values of the exponent r. This is so because "direct hit" events where a deposited atom lands on top of or immediately adjacent to an existing island are known to generate a downward bending of the $N_1(\theta)$ curve for the case of homoepitaxy [13].
[18] F. Family, P. Meakin and J.M. Deutch, Phys. Rev. Lett. 57 (1986) 727;
C.M. Sorensen, H.X. Zhang and T.W. Taylor, Phys. Rev. Lett. 59 (1987) 363.
[19] J.A. Blackman and A. Wilding, Europhys. Lett. 16 (1991) 115.
[20] J.A. Blackman and A. Marshall, J. Phys. A 27 (1994) 725.
[21] L.-H. Tang, J. Phys. (Paris) 3 (1993) 935.